Forests **2015**, *6*, 2125-2147; doi:10.3390/f6062125

OPEN ACCESS

forests

ISSN 1999-4907

www.mdpi.com/journal/forests

Article

Modeling of Two Different Water Uptake Approaches for Mono- and Mixed-Species Forest Stands

Martin Gutsch, Petra Lasch-Born, Felicitas Suckow and Christopher P.O. Reyer *

Potsdam Institute for Climate Impact Research, Telegrafenberg A 62, 14473 Potsdam, Germany; E-Mails: gutsch@pik-potsdam.de (M.G.); lasch@pik-potsdam.de (P.L.-B.); suckow@pik-potsdam.de (F.S.)

* Author to whom correspondence should be addressed; E-Mail: reyer@pik-potsdam.de; Tel.: +49-331-28820725; Fax: +49-331-2882600.

Academic Editor: Steven Jansen

Received: 27 March 2015 / Accepted: 3 June 2015 / Published: 12 June 2015

Abstract: To assess how the effects of drought could be better captured in process-based models, this study simulated and contrasted two water uptake approaches in Scots pine and Scots pine-Sessile oak stands. The first approach consisted of an empirical function for root water uptake (WU1). The second approach was based on differences of soil water potential along a soil-plant-atmosphere continuum (WU2) with total root resistance varying at low, medium and high total root resistance levels. Three data sets on different time scales relevant for tree growth were used for model evaluation: Two short-term datasets on daily transpiration and soil water content as well as a long-term dataset on annual tree ring increments. Except WU2 with high total root resistance, all transpiration outputs exceeded observed values. The strongest correlation between simulated and observed annual tree ring width occurred with WU2 and high total root resistance. The findings highlighted the importance of severe drought as a main reason for small diameter increment. However, if all three data sets were taken into account, no approach was superior to the other. We conclude that accurate projections of future forest productivity depend largely on the realistic representation of root water uptake in forest model simulations.

Keywords: 4C; drought; forest modeling; root water uptake; climate change; model validation

1. Introduction

Changes in environmental conditions due to climate change influence ecological systems. Particularly the projected temperature rise for the next decades may result in a large variation of possible impacts on forest ecosystems [1]. Various model studies have examined the response of forest growth to changing climate conditions to develop future forest management strategies ensuring ecologically viable forest ecosystems [2–5].

Resistance to drought stress is an important factor for the functioning of many forest ecosystems, because of the close relationship between carbon and water cycles in trees expressed by the linkage of stomatal conductance and photosynthesis [6,7]. Climate warming might lead to decreasing water availability due to higher evapotranspiration rates in most European regions [8]. In Mediterranean forests, the morphology, phenology and physiology of trees are well-adapted to recurring drought events [9]. In Central Europe, severe droughts are less frequent and thus the adaptation to drought stress is less distinctive. Especially, the growth of mature forest stands is strongly dependent on water availability during the growing period [10].

In the federal state of Brandenburg, Germany, 70% of forest area is stocked with pure Scots pine (*Pinus sylvestris* L.) stands which are partly being converted to mixed Scots pine-oak stands (*Quercus petraea* [Matt.] Liebl.). The region is characterized by dry climate conditions and soils with low water storage capacity. The vulnerability of Scots pine to severe drought events has already been subject to discussion [11,12]. In addition, the stability of pure Scots pine stands is unclear at the southern and western borders of the distribution area under the condition of continuous temperature increase in the next decades [13].

Therefore, assessing the magnitude of severe drought impacts in the future is essential. Doing so requires the realistic mapping of plant available water, which represents the water supply to tree roots. There are two theories on water flow within trees. First, the *cohesion-tension theory of the ascent of sap* deals with the physics of the sap water movement [14]. Second, the *electrical analogy* describes the water transport within the soil-plant-water continuum by using resistances, capacitances, and water potentials [14].

Process-based forest growth models are suitable scientific tools to study climate impacts and tree responses to droughts [15–18], although drought stress and especially its implications for tree mortality are often not sufficiently covered in these models [19]. Forest canopy models for the soil-plant-atmosphere-continuum as developed by Williams *et al.* [20] link carbon uptake of forest stands to weather conditions and soil properties. They can provide reliable information about the relationships between carbon dioxide uptake, stomatal conductance and transpiration. The water flow is described as an electrical circuit and water uptake of roots is simulated by calculating water flow dependent on the water potential gradient from soil to atmosphere [21–26]. The considered water potentials and resistances depend nonlinearly on the water contents in the particular components along the soil-plant-atmosphere continuum (SPAC). The maximum rate of water supply by roots is determined by the minimum sustainable leaf water potential, the soil conductivity for water flow and the root resistance to water uptake. This approach permits a species-specific characterization of belowground competition in mixed forest stands since modeling of resistances of root water uptake directly depends on relative fine root length densities, a species-specific, measureable parameter. The SPAC-model

predicts varying stomatal conductance so that daily carbon uptake is maximized within the limitations of canopy water and nitrogen availability.

However, the described model by Williams *et al.* [20] is less useful to analyze impacts of extreme weather events (e.g., droughts) on diameter increment and subsequently timber yield of forest stands. For this purpose, models are required that incorporate a carbon allocation module and consider stand development with regard to management and mortality. Economic and ecological sustainability under continuous climate warming can be investigated with these kinds of forest growth models. However, in these models usually a simple function accounts for limited water uptake at decreasing soil water content. They simulate water uptake with an empirical reduction function, which is linearly dependent on soil water content [27,28].

Knowledge about the performance of different water uptake model approaches within a physiological-based forest growth model helps to detect potential severe drought events under future climate scenarios. Furthermore, this knowledge is of major importance for the development of suitable tools for planning adaption strategies as for instance forest conversion. The objective of this paper is to identify the effect of two commonly used water uptake approaches on the simulated amount of plant available water and to assess the resulting effects on tree growth in pure pine and mixed oak-pine forests. Both approaches are implemented in the process based forest growth model 4C (FORESEE—FORESt Ecosystems in a changing Environment) [2] and applied in a simulation study. This simulation study strives to respond to the following questions: (1) Are there differences between both approaches regarding the water supply from the roots? (2) How well can drought years, observed by annual tree ring analyses, be reproduced by the different water uptake approaches? (3) Is there an approach that performs best regarding different validation data sets?

Due to the complexity of comparing these two approaches with regard to direct and indirect effects on different model output variables (e.g., soil water limitation → reduction of transpiration → reduction of diameter increment), we here employ three different data sets to discuss the two model approaches at several time scales relevant for tree growth. The data sets include (1) daily transpiration and (2) soil water content measurements over a short-term period, which we use to directly evaluate root water uptake; and (3) annual tree ring data, serving as a long-term validation archive for severe drought events, which constitute an indirect link to root water uptake impacts [29]. We initialize the model for each forest stand with the soil description available for that stand. Then, we run the model with the two different water uptake approaches for each stand and only the model formulation with regard to water uptake is different.

2. Material and Methods

2.1. Forest Growth Model 4C

The physiologically-based forest growth model 4C has been used to simulate growth, water, and carbon budget of trees and soils under current and projected climate condition and to analyze the long-term growth behavior of forest stands. 4C was applied in different studies and validated across a wide range of forest sites [2,5,30,31]. Modeled processes are based on eco-physiological experiments, long-term studies of stand development, and physiological relationships [32] at tree and stand level.

Establishment, growth, and mortality are explicitly modeled on individual patches for which homogeneity is assumed. The model simulates tree species composition, forest structure, leaf area index as well as ecosystem carbon and water balances. The cohort structure of simulated tree growth enables a detailed analysis from stand to single-tree level, whereas a cohort represents trees of same species, age and dimensions. The length of the growing season is provided by a species-specific phenological model with prohibitors and inhibitors [33]. The photosynthesis submodel is based on the photosynthesis model of Haxeltine and Prentice [32]. The photosynthesis is calculated under the assumption of unlimited water and nutrient supply and then reduced based on actual nutrient and water limitations. Reductions of photosynthesis by water are represented through a drought reduction factor R_{drind}, calculated as the ratio between soil water supply and tree water demand, thus following the physiological logic of the model. The model variable R_{drind} is not a static parameter but dynamically calculated in the model as a result of the link between photosynthesis and water balance of the tree. We analyze it in this study to compare both water uptake approaches.

For simulating water and carbon balances in the forest soil, a multilayered soil model is implemented in 4C. Water balances are calculated using a bucket model approach [34,35]. The surplus water above field capacity percolates out of the last soil layer and thus represents deep soil water infiltration. The soil column is divided into different layers with optional thickness according to the horizons of the soil profile. Each layer, the humus layer and the deeper mineral layers, is considered homogeneous concerning its physical and chemical parameters. Water content and soil temperature of each soil layer are estimated as functions of the soil parameters, air temperature, and stand precipitation and control the decomposition and mineralization of organic matter. The water input to the soil is equivalent to the throughfall (precipitation minus interception). The interception is determined by the interception storage and the potential evapotranspiration [36]. The interception storage is calculated from a leaf area index that is weighted by a species-specific storage capacity. The calculation of the soil temperature of each soil layer is described by Grote and Suckow [27].

2.2. Modeling Water Uptake

2.2.1. Empirical Water Uptake Approach—WU1

The water uptake approach (WU1) assumes the water uptake of a tree cohort to be controlled by the transpiration demand, the relative amount of fine roots of a tree cohort in a specific soil layer relative to the total amount of fine roots in this soil layer, the available water above the wilting point, W_s^{WP}, and a reduction function [37]. The reduction function f_{res} is based on the assumption that optimal water uptake only occurs if water content, W_s, is in range of ±10% of the field capacity, W_s^{FC}. Hence, WU1 follows a demand-approach that looks stepwise from the upper to the lower soil layer for the required amount of water. The water demand of a tree cohort is calculated from the potential evapotranspiration and the canopy conductance with regard to photosynthesis. This demand is met by the supply of soil water, calculated from water content of the soil layers reduced by a water content dependent reduction factor (Figure 1).

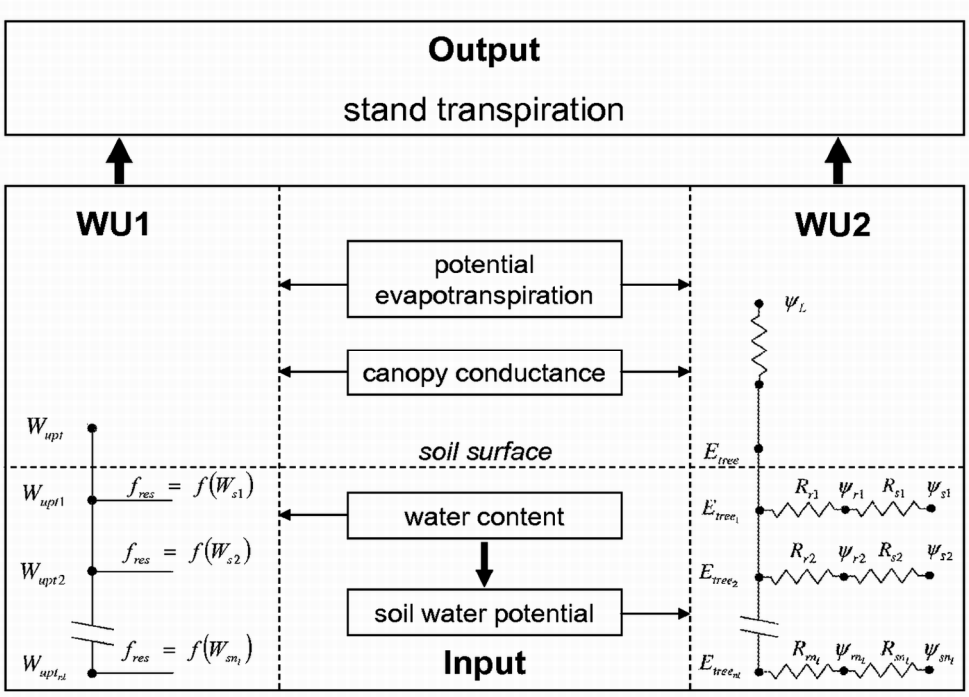

Figure 1. Schematic overview of the simulated components for WU1 and WU2. With W_{upt} and E_{tree} = sum of water uptake of a tree over n_l number of soil layers, W_s = soil water content, R_r = root resistance, R_s = soil resistance, ψ_L = leaf water potential, ψ_r = root water potential, ψ_s = soil water potential.

The water supply by roots W^c_{upt} [mm] per soil layer is calculated by WU1 as follows:

$$W^c_{upt} = W_s \cdot f_{res} \tag{1}$$

where Ws is the soil water content [mm] of the respective soil layer. The reduction factor f_{res} that implies the reduced water uptake at water contents besides the optimum is simulated as follows:

$$f_{res} = \begin{cases} 1 - \dfrac{0.9 \cdot W_s^{FC} - W_s}{0.9 \cdot W_s^{FC} - W_s^{WP}}, W_s < 0.9 \cdot W_s^{FC} \\ 0.3 + 0.7 \cdot \dfrac{W_s^{sat} - W_s}{W_s^{sat} - 1.1 \cdot W_s^{FC}}, W_s > 1.1 \cdot W_s^{FC} \\ 1, otherwise \end{cases} \tag{2}$$

where W_s^{sat} is the saturated water content of soil layer, W_s^{FC} is the soil water content at field capacity and W_s^{WP} is the soil water content at wilting point.

2.2.2. Process-Based Water Uptake Approach—WU2

The second approach for water uptake (WU2) was developed by Campbell [21] and describes the water uptake process along a soil-plant-atmosphere continuum (SPAC). The algorithm has been implemented in 4C to simulate water uptake based on the water potential gradient between leaf and soil analogous to electricity flow. The water flows from soil through xylem into the leaves and

evaporates through the stomata into the atmosphere. Figure 1 illustrates the simulated time dynamic components within the applied water uptake approach. Two major resistances in the system are calculated: the soil resistance (Equation (7)) and the root endodermis resistance (Equation (4)). Axial resistances within roots and xylem resistances within the stem are not considered in the model and the leaf resistance is constant over time and tree species. The potential gradient with the lowest water potential in the leaves and the highest water potential in the soil is the driver of the water flow in trees. The root resistance in a soil layer is inversely proportional to the relative length of fine roots in that layer. In the following we show the key equations from the original source of WU2 [21]. The list of parameters of WU2 is provided in Table S1.

WU2 calculates the water supply of the roots W^c_{upt} for cohort c with water content of the soil W_s and transpiration of one tree from cohort c, which is multiplied by the number of trees within the cohort $N_{tree}{}^c$.

$$W^c_{upt} = \min\left(N^c_{tree} \cdot E_{tree}, W_s\right) \tag{3}$$

E_{tree} is the transpiration flow within the soil-plant-atmosphere continuum of the single tree of cohort c.

The transpiration or water uptake of a tree E_{tree} over all soil layers, without considering xylem resistance, is calculated from the soil water potentials ψ_{si}, the xylem water potential ψ_{xri} and the soil and root resistances R_{si} and R_{ri} of all soil layers n_l.

$$E_{tree} = \sum_{i=1}^{n_l} \frac{(\psi_{si} - \psi_{xri})}{(R_{si} + R_{ri})} \tag{4}$$

The first major resistance R_{ri} (root resistance) is directly proportional to the total root resistance $R_r{}^{tot}$ and inversely proportional to the fine root length density L_i [m·m^{-3}] in soil layer i.

$$R_{ri} = \frac{R_r^{tot} \cdot \sum_{i=1}^{n_l} L_i}{L_i} \tag{5}$$

The second major resistance R_{si} (soil resistance) is calculated once per day for every soil layer i by a simplified approach from the fine root length density L_i and the conductivity of root (k_r) and soil (k_s).

$$R_{si} = \frac{H_i}{k_{si}} \tag{6}$$

with:

$$H_i = \frac{(1-n)ln(\pi r_r^2 L_i)}{(4\pi L_i \Delta z_i)} \tag{7}$$

where r_r is the fine root radius, Δz_i the thickness of soil layer i and n a dimensionless parameter. We calculated water uptake with low, medium and high total root resistance (WU2-low, WU2-medium, and WU2-high; Table S1). The soil water potentials were calculated on the base of pedotransfer functions from the actual water content [38].

2.3. Forest Stands and Site Conditions

The simulation experiments were conducted on four different forest sites in Germany. We choose two mono-species Scots pine (*Pinus sylvestris* L.) stands (P1, P2) and two mixed Scots pine-oak (*Quercus petraea* [Matt.] Liebl.) stands (M1, M2) located in the lowlands of northeastern Germany. P1 and P2 are part of the network of long-term forest monitoring sites within the ICP Forest program of the UN-ECE.

For the short-term validation, we accessed initialization data for the P1 and P2 stand from 1994 (Table 1). The simulation period for long-term validation starts in 1951. Since there were no observed stand data for the start year of simulation in 1951, we used available data of inventories from 2006 (M1, M2) and 2004 (P1, P2) to generate stands for 1951 from yield table data. We assumed stability in the site quality index (mean dominant tree height at age 100) and in the share of basal area in mixed stands and initialized the stands on the base of tree age, mean height, mean diameter and basal area from the yield table (Table 1).

Table 1. Stand data for initialization in 1951 and 1994, respectively (d_g = mean tree diameter at breast height, h_g = mean tree height).

		1951				1994			
		Age (years)	**d_g (cm)**	**h_g (m)**	**Stock (m^3)**	**Age (years)**	**d_g (cm)**	**h_g (m)**	**Stock (m^3)**
P1	pine	18	9.0	13.7	209	62	29.8	25.9	458
P2	pine	29	10.5	14.0	205	73	28.3	24.3	347
M1	pine oak	85	31.8	25.0	258				
		85	20.9	20.0	136				
M2	pine oak	65	24.8	23.1	159				
		70	21.2	22.4	239				

Soil data were available from soil inventories. The soil characteristics differ between the pure and the mixed stands. In particular, the sum of plant available water is much greater for the mixed stands (Table 2).

Table 2. Soil characteristics from soil inventory (W_s^{FC} = Sum field capacity, W_s^{AW} = Plant available water at maximum rooting depth, C/N = Carbon Nitrogen ratio total soil, p_s = range sand fraction, p_c = range clay fraction).

Site	**Soil Type**	**Soil Depth (cm)**	**W_s^{FC} (mm)**	**W_s^{AW} (mm)**	**C/N**	**p_s (%)**	**p_c (%)**
P1	brunic arenosol	270	217	119	22	90–100	0–5
P2	brunic arenosol	255	237	93	21	50–100	0–17
M1	brunic arenosol	308	526	369	21	91–98	1–4
M2	brunic arenosol	305	607	395	15	75–97	2–9

2.4. Climate Data

The climate data are provided by climate stations, which are located nearby the forest stands. These climate data include daily measurements of weather parameters (temperature, precipitation, radiation, air humidity, vapor pressure, wind velocity) from 1951–2006 (Table S2). In the case of the pure pine stands (P1, P2), climate data of a mobile climate station next to the forest stand was also available from 1996–2004. For these stands, we merged the long time series of the permanent climate station with the short but more precise one of the mobile climate station wherever possible.

The climate conditions at the forest sites represent the subcontinental climate prevailing in Brandenburg with low precipitation in the growing season but slightly differ in precipitation and temperature (Table 3).

Table 3. Climatic characterization of forest sites on the base of permanent climate stations (T_y = yearly average temperature, T_g = growing season (April–September) average temperature, P_y = average annual sum of precipitation, P_g = growing season (April–September) average sum of precipitation.

Site	T_y (°C)	T_g (°C)	P_y (mm)	P_g (mm)
P1	8.1	13.8	600	344
P2	8.5	14.7	550	309
M1	8.5	15.2	531	255
M2	8.9	16.2	521	267

2.5. Measured Data

2.5.1. Xylem Sap Flow Data

Tree canopy transpiration was estimated by sap flow measurements in 10 representative pine trees of stand P1 using the constant heating method based on Granier [39]. The method is described in detail for this dataset by Lüttschwager *et al.* [40]. The stand sap flow was calculated as the product of average sap flow density and stand sapwood area that was estimated by stand inventory and sapwood area in the sample trees. The measurements were taken from June 1998 until October 1999. The aggregated stand transpiration estimated from the measured data was compared with simulated stand transpiration (Table 4).

Table 4. Summary of data and measurement periods available for each forest stand considered in this study.

Site	Data	Period	Source
P1	• sap flow	06/1998–10/1999	[40]
	• time domain reflectometry (TDR)	1997–2004	[41–43]
	• tree rings	until 2004	[44]
P2	• time domain reflectometry (TDR)	1997–2004	[41–43]
	• tree rings	until 2004	[44]
M1	• tree rings	until 2006	[45]
M2	• tree rings	until 2006	[45]

2.5.2. Soil Water Content

The volumetric soil water content was taken from [41–43] and calculated using the time domain reflectometry (TDR) measurements at the P1 and P2 sites. The TDR tubes were installed in three different soil depths (P1: 20, 70, 250 cm and P2: 20, 50, 250 cm). The observation period lasted from 1997 until 2004 (Table 4).

2.5.3. Tree Ring Data

The growth dynamics of the trees was measured on the base of annual ring widths taken from increment cores. In each case, two increment cores were extracted from 20 dominant pines and 20 dominant/subdominant oaks at the M1 and M2 sites in 2006 [45]. At P1 and P2, only average annual ring width time series until 2004 for dominant pine trees were available [44]. For the comparison between simulated and measured ring widths, we also calculated the average annual ring width time series at the mixed forest stands M1 and M2 (Table 4).

2.6. Validation Procedure

The validation of the different model approaches to simulate water uptake were executed with different variables available from the different measurement periods. The processes that are important for tree growth are simulated at different time scales. The soil water balance is simulated with a daily time step and, consequently, the validation is also done with daily data. The short-term validation with the transpiration measurements on P1 encompasses one and a half years and the soil water measurements on P1 and P2 eight years. The annual diameter increment is simulated at the end of the year when the carbon is allocated to the stem. Therefore, the long-term validation is executed with annual data with the tree ring chronologies from 1951–2004 (P1, P2) and 1951–2006 (M1, M2), respectively.

The average annual ring increment for each species and site were used to derive index series through normalization. The index values were calculated in two steps. Firstly, an autoregressive model converts increment values into index values:

$$I'_t = \frac{rw_t}{(a + b \cdot rw_{t-1})} \tag{8}$$

where rw_t is the ring width and rw_{t-1} is the ring width of previous year, a and b are empirical parameters.

Secondly, a linear regression minimizes the tree age impacts:

$$I_t = \frac{I'_t}{(c + d \cdot t_{age})} \tag{9}$$

where t_{age} is the tree age, c and d are empirical parameters.

We compared the index time series of simulated and observed diameter growth by considering four criteria. The first criterion is the *Pearson* correlation coefficient r (Equation (3)):

$$r = \frac{\sum_{i=1}^{n}(X_i - \bar{X})\,(Y_i - \bar{Y})}{\sqrt{\sum_{i=1}^{n}(X_i - \bar{X})^2 \sum_{i=1}^{n}(Y_i - \bar{Y})^2}} \tag{10}$$

where X_i is the ith simulated value (i = 1, .., n), $\bar{X}$ is the arithmetic mean of simulated values, Y_i is the i-th measured value (i = 1, .., n), $\bar{Y}$ is the arithmetic mean of measured values.

For the soil water content we used the coefficient of determination R^2 between simulated and measured values:

$$R^2 = \frac{\sum_{i=1}^{n}(\hat{Y}_i - \bar{Y})^2}{\sum_{i=1}^{n}(Y_i - \bar{Y})^2} \quad (11)$$

where $\hat{Y}_i$ is the ith estimated value of the regression between simulated and measured values, $\bar{Y}$ the arithmetic mean of simulated values, Y_i the ith simulated value and n the number of pairs of simulated and measured values.

The sensitivity index (SI) indicates the year-to-year fluctuations of ring widths [44]. Sensitivity index is calculated using the following equation:

$$SI = \sum_{i=2}^{n} \frac{(x_{i-1} - x_i)}{(x_{i-1} - x_i) \cdot 0.5} \quad (12)$$

The third criterion is the "Gleichläufigkeit" score G_{xy} of two tree ring index series x_i and y_i (i = 1, …, n) and is defined by:

$$G_{xy} = \frac{1}{n-1} \sum_{i=2}^{n} sign(x_i - x_{i-1}) \cdot sign(y_i - y_{i-1}) \quad (13)$$

with:

$$sign(z) = \begin{cases} 1 & z > 0 \\ 0 \ if & z = 0 \\ -1 & z < 0 \end{cases} \quad (14)$$

This index counts how well the two series have followed each other over the years. The last criterion is a drought index (*DI*) to detect marker years with small diameter growth due to water shortage. Following Schröder *et al.* [45], we defined a marker year as a year where the diameter increment of a year is at minimum 10% above or below the increment of the previous year. Thereafter, only the lower increments were used to filter out the drought years. Because complex interactions between climate, management and diameter growth can confound the effect of drought, we filtered out years where remarkably low diameter increment should mainly be caused by water shortage. For this filtering, a cluster analysis was performed on the base of the variables minimum water content in the soil, climatic water balance of the year and number of ice days (T_{max} < 0 °C). At each site, the classification of the marker years to three clusters was based on the Euclidean distance. As a result, marker years with dry conditions could be separated from marker years with a strong winter and marker years with wet conditions. The resulting drought years (Table S3) fit well to reported drought years in the northeastern lowlands of Germany. The cluster analysis was conducted with the software package "*cluster"* available for *R* [46,47]. The drought index, *DI*, is then calculated as the percentage concurrence of observed and simulated drought years.

2.7. Statistical Analysis

To find an over all result of the performance of the water uptake approaches related to the annual diameter increment we aggregated the four criteria described above into one metric. Since all four criteria can be assessed with a scale from 0% to 100%, they were standardized to allow calculating a mean value for the water uptake approaches. Hereby, the standardization of the four criteria is as follows:

criteria I $r^* = r \times 100$ (if $r < 0$; $r^* = 0$)
criteria II $G_{xy}^* = G_{xy}$
criteria III $SI^* = 100 - (|SI_{sim} - SI_{meas}|)/SI_{meas} \times 100)$
criteria IV $DI^* = DI$

The asterisk indicates the standardized criterion and a value of 100% means perfect compliance with the criterion of the measured index time series.

The Tukey test (tukeyHSD, package *stats*) [47] was used to test for significant differences between the four average compliance values of the four water uptake approaches WU1, WU2-low, WU2-medium, and WU2-high. It is a nonparametric test for multiple comparisons. The performance of the water uptake approaches simulating stand tree transpiration and soil water content at a specific soil depth was evaluated using the coefficient of determination R^2 between simulated and measured values (Equation (11)). The coefficient of variation (*CV*) as the ratio between the standard deviation and the mean value was calculated to compare variation in simulated and observed soil water content. The statistical analyses were conducted with equations implemented in 4C and with the package *"base"* statistical software *R* version 2.10.0 [47].

3. Results

3.1. Daily Xylem Sap Flow

The daily stand transpiration rates simulated with WU1 are higher than the observed stand transpiration from the xylem sap flow data. The transpiration simulated with WU2-medium was closest to the simulated transpiration with WU1. The simulation with WU2-high leads to a decrease in transpiration that is lower than observed transpiration but closer to the observed values than the simulations with WU1, WU2-low and WU2-medium (Figure 2).

There is a general overestimation of daily transpiration for WU1, WU2-low, and WU2-medium by roughly twice of the observed values. The scatter plot also shows that there are many days where no transpiration is simulated but measured (simulated $T_{stand} = 0$ *versus* measured $T_{stand} > 0$). The best correspondence of simulations and observations is shown for WU2-high (Figure 3).

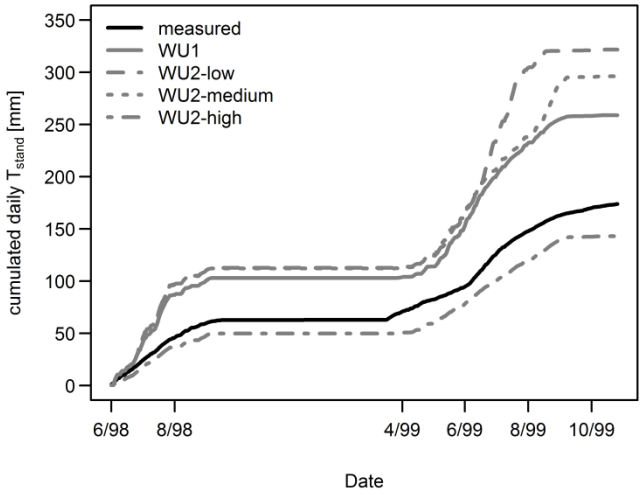

Figure 2. Measured and simulated transpiration of P1 site. Simulated transpiration with WU2 involves three different values for root resistance (low, medium, high).

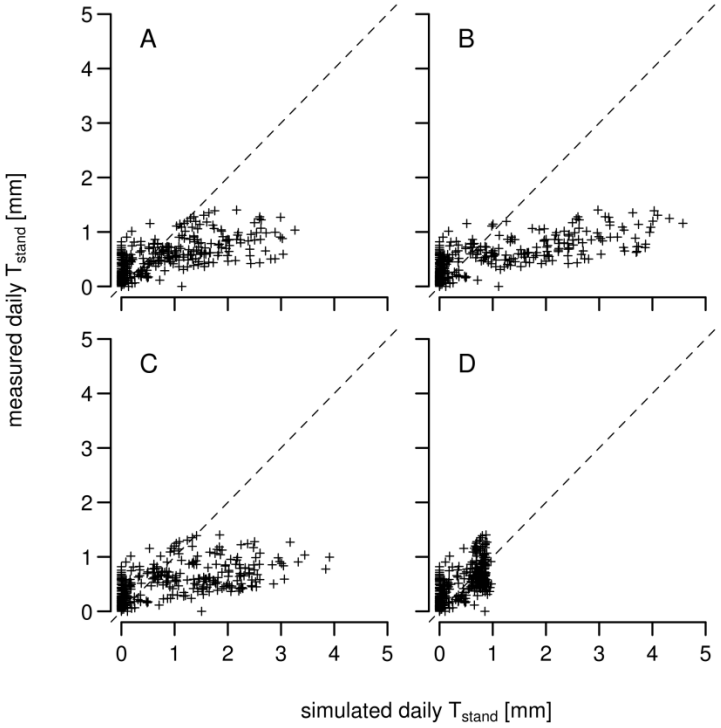

Figure 3. Measured and simulated daily transpiration at P1 site for all both water uptake approaches and root resistances from June 1998 until October 1999 ((**A**) = WU1; (**B**) = WU2-low; (**C**) = WU2-medium; and (**D**) = WU2-high).

3.2. Daily Soil Water Content

The comparison between observed and simulated soil water content on the basis of the R^2 coefficient showed the best agreement of WU1 in all three soil depths at P1 (Table 5). However, the variation in the soil water content in 250 cm soil depth is much lower than observed. The opposite applies for WU2-low and WU2-medium. The R^2 value is mostly lower than with WU1 but the CV value is higher (WU2-low and 250 cm soil depth) or close to the observed values.

Table 5. Statistical analyses between mean simulated and observed volumetric soil water content from 1997–2004 at P1. *CV* is the coefficient of variation. R^2 is the coefficient of determination between simulated and measured water contents.

	Soil Depth	***R^2***	***Mean Soil Water Content [%]***		***CV of Soil Water Content***	
	[cm]		**Simulated**	**Measured**	**Simulated**	**Measured**
WU1	20	0.50	14.75	15.32	0.17	0.23
	70	0.41	9.95	10.90	0.12	0.11
	250	0.55	8.55	11.88	0.12	0.25
WU2-low	20	0.51	14.37	15.32	0.23	0.23
	70	0.35	9.82	10.90	0.14	0.11
	250	0.36	7.56	11.88	0.38	0.25
WU2-medium	20	0.52	14.57	15.32	0.20	0.23
	70	0.38	9.97	10.90	0.12	0.11
	250	0.31	8.36	11.88	0.23	0.25
WU2-high	20	0.32	15.65	15.32	0.10	0.23
	70	0.43	10.43	10.90	0.08	0.11
	250	0.07	9.15	11.88	0.07	0.25

WU1 led to water contents that fitted well to the observed water content measurements in its general pattern (Figure 4A,B). As observed, the water content in upper soil layers is much lower in relatively dry years (e.g., 1999 and 2003). This is accompanied by a sharper decrease of water content in the deeper soil layers. However, the magnitude of this decrease is lower than observed, which causes a much lower variation than the observed variation of soil water content (Table 5). The results in water content of the upper soil layer with WU2-low were similar to the results of WU1. Though, the simulated minimum soil water content of the upper soil layers in a year is lower than the observed water content and also lower than simulated with WU1 (Figure 4C). There was a big difference between simulated and observed water content in the deeper soil layers where the model simulated that almost all water could be extracted by the trees in dry years (Figure 4D).

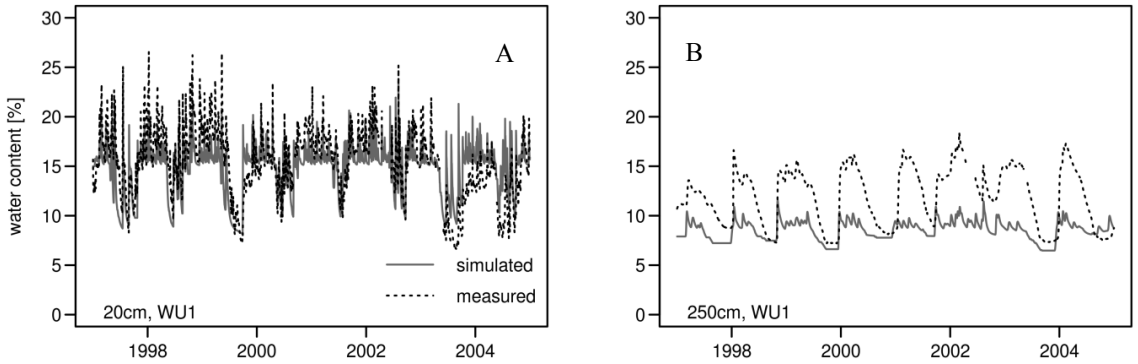

Figure 4. *Cont.*

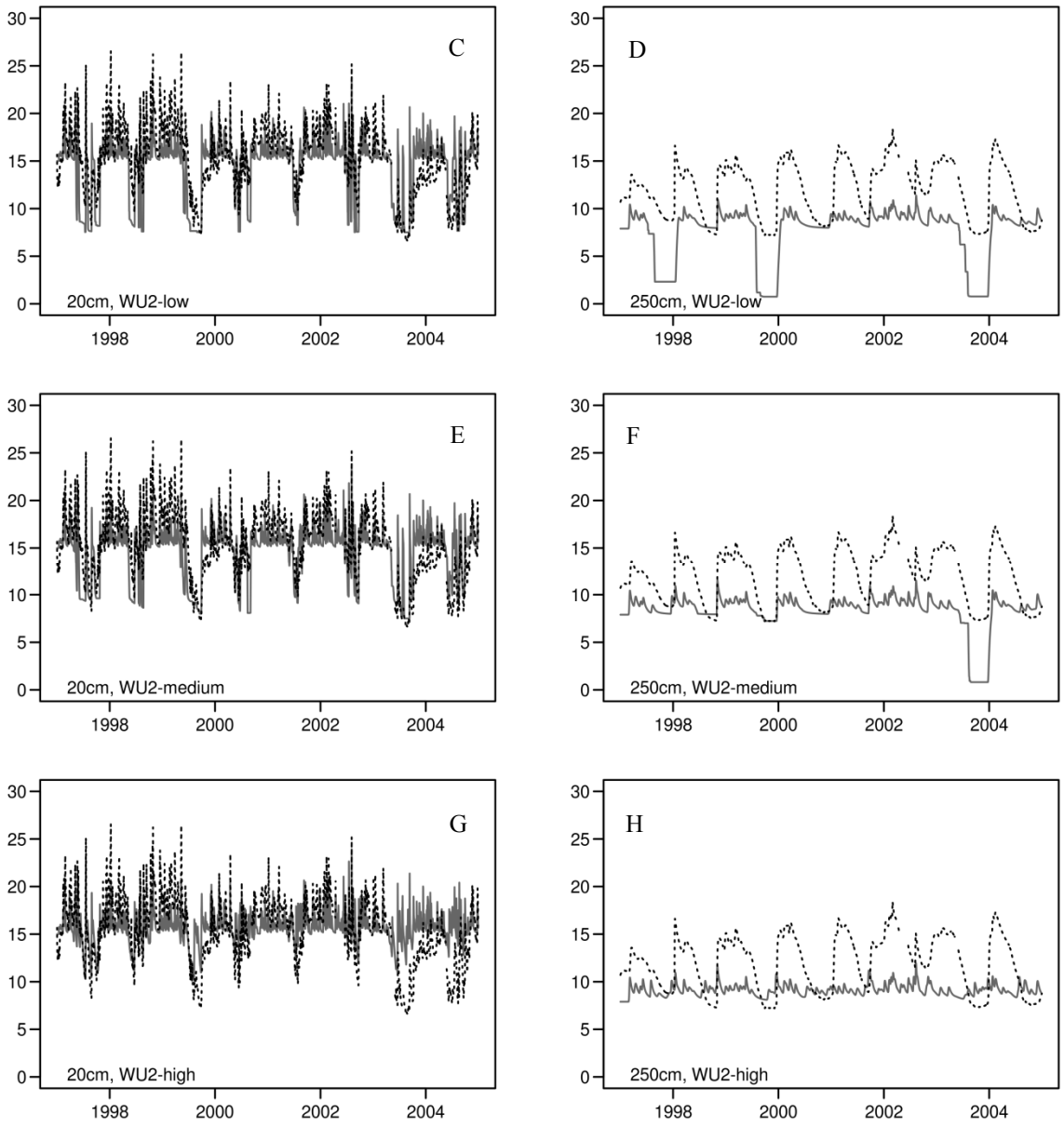

Figure 4. Volumetric soil water content at P1. The figure shows daily data for the upper soil layer (left panels; 20 cm) and lower soil layer (right panels; 250 cm). ((**A**,**B**) = WU1; (**C**,**D**) = WU2-low; (**E**,**F**) = WU2-medium; and (**G**,**H**) = WU2-high).

With WU2-medium, the simulated soil water content in upper soil layers is closest to the observed values in comparison to all other simulations but WU1 performs only slightly worse (Figure 4E; Table 5). The approach WU2-medium led to less water extraction in deep soil layers and subsequent lower variation in water content. In the relative dry year 2003 almost all of the stored water was extracted (Figure 4F).

The WU2-high led to lower transpiration and therefore to higher water content in the soil. In the upper soil layers the simulated soil water content is higher than the observed water content in the growing season and the simulated water content with WU1 (Figure 4G). There was a big difference between simulated and observed water content in the deeper soil layers where almost no water is extracted by the trees in the model simulation (Figure 4H).

3.3. Annual Tree Ring Data

The mean annual drought reduction factor R_{drind} was lower if water uptake was simulated with the WU2 approaches (Figure 5). The highest reduction in photosynthesis due to water stress is simulated as occurring with WU2-high.

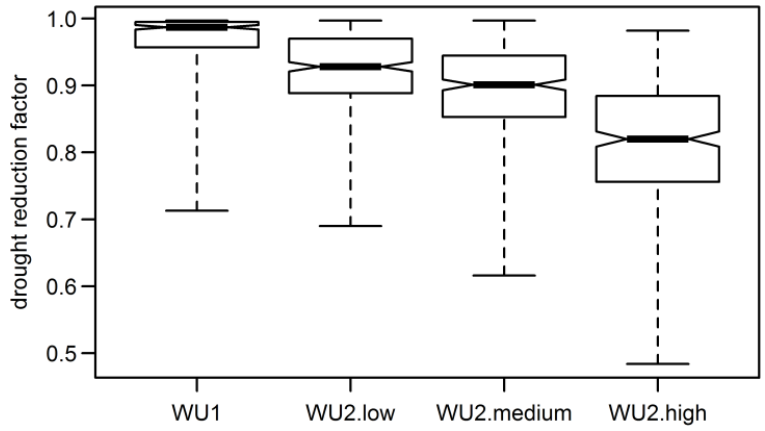

Figure 5. Box plots (lower whisker = lowest extreme, lower hinge = first quartile, median, upper hinge = third quartile, upper whisker = highest extreme, the notch represents the standard error of the median [48]) of the mean annual drought reduction factor R_{drind} in 4C over all sites and tree species for the different water uptake approaches. The time period of the average was from 1951–2006 (M1, M2) and 1951–2004 (P1, P2), respectively.

The comparison of simulated and observed diameter growth on the base of the index time series offered a more differentiated picture. The four assessment criteria show a general trend to better performance of WU2 (Table S4). At most sites, either WU2-medium or WU2-high lead to the highest standardized criteria values.

3.4. Aggregated Datasets

An over all comparison to sites and standardized criteria, WU2-high had the highest mean compliance. The Tukey test indicated no significant difference between the different water uptake approaches (Table 6).

Table 6. Mean compliance of standardized index values and adjusted (with respect to multiple comparisons) *p*-values of a *Tukey*-test (significant difference at $p < 0.05$).

Model	Mean Compliance	WU2-Low	WU2-Medium	WU2-High
		47.3	**54.6**	**56.7**
WU1	**41.9**	0.81	0.16	0.08
WU2-low	**47.3**		0.62	0.42
WU2-medium	**54.6**			0.99

4. Discussion

4.1. Water Uptake and Root Resistance

The assumed total root resistances of 4.0×10^6, 9.0×10^6 and 4.0×10^7 ($m^4 \cdot s^{-1} \cdot kg^{-1}$) were set according to the value of 4.6×10^6, which was used by Campbell [21] for tomato plants. To check if these values are also realistic for trees and for a better comparison with root resistance values from the literature we converted all values to total root resistance per tree. This conversion shows that the estimated total root resistance of our study ranges from 2.3×10^4 to 2.3×10^5 (MPa $s \cdot m^{-3}$), which is in the range of the values reported by Coners [49] and Williams *et al.* [25] for forest trees (ranging from 1.8–8.7×10^4 and 2.5×10^5 (MPa $s \cdot m^{-3}$), respectively). In our study, this parameter showed a high sensitivity. However, due to the complexity of physical and chemical processes that control the root resistance and missing fine root data it was not possible to select a "best" value for our model study.

4.2. Short-Term Performance of Root Water Uptake Approaches

At the daily level there were large discrepancies between simulated and observed cumulated transpiration measured by the sap flow method (Figure 2). According to Kostner *et al.* [50] (1996), they cannot be explained by the estimation error in the aggregation of transpired water from single-tree to the stand since this estimation error does not exceed 10% with ten investigated trees in an even aged mono-specific stand. On the other hand, Wilson *et al.* [51] reported much lower values of stand transpiration measured by the sap flow method than by eddy covariance and water catchment methods. They explained the discrepancies with scaling errors of instrumented trees to the stand due to diversity in stand species composition and ring porous trees. Therefore, in case of P1, the sap flow method should give reliable values for tree transpiration but with some uncertainty about the tendency to underestimate transpiration. Some problems occurred with days where no transpiration was simulated but measured (Figure 3), which can be explained with the delay in the beginning of simulated transpiration in spring of the year 1999. The higher root resistance in WU2-high led to lower daily tree transpiration rates with a maximum of 1 mm per day (Figure 3D). Furthermore, measured daily transpiration values did not exceed 1.5 mm and were seldom above 1 mm. In comparison to other reported maximum values around 3–4 mm per day [52–54] the simulated values with WU2-high, but also the measured values, seem to be too low.

In contrast to the overestimated transpiration by WU1 and WU2-low the simulated water content were close to the observed water content for these approaches for all soil depths (Table 5, Figure 4A–D). Especially, the soil water content of the lowest layer (250 cm depth) was simulated with the same intra-annual pattern of a water content decrease during summer and a clear increase during winter time between 1997 and 2004. In WU1, this is obviously caused by the water demand and the ability of the approach to satisfy this demand with the water from all soil layers. In the case WU2-low the water supply was not limited due to low root resistance in this layer. *Vice versa*, since lower tree transpiration was simulated by WU2-medium and WU2-high, the soil water content was much higher than observed (e.g. Figure 4E–H). During the very dry and heat summer of 2003 WU2-high simulated a higher water content than measured in the upper soil layer (Figure 4G). Also, in the lowest soil layer,

the simulated soil water content did not show the seasonal pattern of variation. This was caused by the high root resistance, which in combination with low root length density led to a high limitation in water uptake.

These findings may lead to the conclusion that the approach, which described transpiration in the best way, did not meet the measured soil water content and *vice versa*. This result can be explained by missing understorey vegetation transpiration in the stand transpiration measurement. According to Lüttschwager [40], understorey vegetation participates with 30%–40% to the total stand transpiration in similar pure pine stands. 4C simulates understorey vegetation as a simple species-independent leaf-area layer and its fraction of the total stand transpiration was in each case smaller than 10%. This results in an underestimation of simulated understorey vegetation transpiration. If understorey vegetation were more realistic the tree transpiration would drop and simulated transpiration of WU1, WU2-low and WU2-medium would be lower. WU2-high would not drop much since soil water is still available. However, higher understorey vegetation transpiration would decrease the soil water content, thus, rendering WU2-medium and WU2-high more realistic with regard to soil water content measurements.

4.3. Effect of Root Water Uptake Approach on Diameter Growth

At the annual level, considering tree ring data of different quality for P1 and P2 (only average annual ring width time series) and M1 and M2 (individual tree ring time series), there was a general trend to a better performance of the WU2 approach. On the bases of the mean compliance to over all criteria, the best results were found with WU2-high (Table 6). In this case the average drought reduction factor R_{drind} had the lowest values (Figure 5) and additionally, the drought index, *DI*, the correlation and the "Gleichläufigkeit" G_{xy} between the index series reached the highest values for WU2-high or WU2-medium (Table S3). Lower values of R_{drind} resulted in a higher reduction of net primary production and subsequently of the diameter growth due to drought stress. This corresponds to a better correspondence between observed and simulated drought years, indicated by *DI*. For both tree species and for all sites the sensitivity index (SI) criterion, calculated for the tree rings simulated with WU2, corresponded better to the SI of the measured tree rings in most cases as well (Table S3). Considering high sensitivity of ring widths as a clear indicator of stress conditions [44], this finding supports the idea that the higher drought stress simulated with WU2 led to a more realistic performance of 4C (Figure 5).

The diameter growth of most tree species in temperate regions is less sensitive to droughts late in the growing season, which is not accounted for in growth models if allocation is simulated with an annual time step [55]. 4C works with such an annual time step of allocation and this may lead to an overestimation of drought stress impact on diameter growth. A better match of the measured index time series could be achieved if 4C would allocate the assimilated carbon at shorter time scales.

There were no significant differences in the criteria between the two tree species and different forest composition (mono *vs.* mixed stands) for the four sites. This supports the assumption of similar growing conditions at these sites. Here, water availability is a limiting factor for tree growth. It seems that with WU1, the simulated drought reduction factor was not capable to describe the water stress at the sites. WU2 leads to higher water stress and better agreement to the measured tree ring index time

series depending on the root resistance. This is in accordance with findings that reductions in sap flow over time and resulting drought stress could be best explained by rising soil-root resistance [25,26]. However, in our study this does not lead to better compliance with measured daily transpiration and soil water content data at the same time.

5. Conclusions

This paper integrated two water uptake approaches—an empirical one and a process-based one—in a process-based forest growth model and evaluated their performance in Scots pine and Scots pine-Sessile oak stands in Germany. We firstly assessed whether there are main differences between the two water uptake approaches regarding the water supply from the roots. We show that the main difference between them is the nonlinear relationship between soil water content and soil water potential, which determines the soil water resistance. This induces different root water uptake in the process-based approach in comparison to the empirical one, which is linearly dependent on a soil water content reduction factor. The study also showed the high influence of the assumed total root resistance on water uptake. In the empirical water uptake approach, the modeled root distribution and, consequently, root length densities in different soil layer have negligible effects on water uptake. In contrast, the modeled root length densities lead to high water uptake limitations in the process-based approach with high total root resistance.

Secondly, we analyzed how well drought years could be reproduced by the different water uptake approaches. We found the highest compliance between observed and simulated drought years in the process-based water uptake approach with high total root resistance.

Finally, we assessed whether there was one approach that performed best regarding the different validation data sets. This study shows that there is not one approach that performs best regarding all three validation data sets. For a better validation of both approaches, it would be necessary to include measurements of root length densities and water uptake rates of fine roots on the same site. However, despite these further data requirements for more advanced model evaluation, this study clearly indicates that forest process-based models aiming at simulating drought conditions require further improvement in terms of model formulations and validation of different processes at various time scales. Further, we highlight the importance of a realistic modeling of understorey vegetation transpiration, especially in mature pine stands with high understorey vegetation cover.

Acknowledgments

We are grateful to Steven Jansen for the invitation to submit our work to this Special Issue. We would like to thank Jens Schröder (LFE Eberswalde) and Dietmar Lüttschwager (ZALF Müncheberg) for making the validation data available and Michael Krause for helpful comments on the manuscript. Most part of the presented study was funded by the BMBF project OakChain and the EFI Scholarship for scientific staff exchange. We thank Alexander Eden for technical assistance and two reviewers for their valuable comments.

Author Contributions

Martin Gutsch conceived the study and implemented the new water uptake approaches in 4C with the help of Petra Lasch-Born and Felicitas Suckow, Martin Gutsch performed the model runs and analysis. All authors interpreted the results and wrote the paper.

Conflicts of Interest

The authors declare no conflict of interest.

References

1. Alcamo, J.; Moreno, J.M.; Nováky, B.; Bindi, M.; Corobov, R.; Devoy, R.J.N.; Giannakopoulos, C.; Martin, E.; Olesen, J.E.; Shvidenko, A.; *et al*. Europe. In *Climate Change 2007: Impacts, Adaptation and Vulnerability*; Contribution of Working Group II to the Fourth Assessment Report of the Intergovernmental Panel on Climate Change; Parry, M.L., Palutikof, J.P., van der Linden, P.J., Hanson, C.E., Eds.; Cambridge University Press: Cambridge, UK, 2007; pp. 541–580.
2. Lasch, P.; Badeck, F.W.; Suckow, F.; Lindner, M.; Mohr, P. Model-Based analysis of management alternatives at stand and regional level in Brandenburg (Germany). *For. Ecol. Manag.* **2005**, *207*, 59–74.
3. Lindner, M.; Cramer, W. German forest sector under global change: An interdisciplinary impact assessment. *Forstwiss. Cent.* **2002**, *121*, 3–17.
4. Pussinen, A.; Nabuurs, G.J.; Wieggers, H.J.J.; Reinds, G.J.; Wamelink, G.W.W.; Kros, J.; Mol-Dijkstra, J.P.; de Vries, W. Modelling long-term impacts of environmental change on mid- and high-latitude European forests and options for adaptive forest management. *For. Ecol. Manag.* **2009**, *258*, 1806–1813.
5. Reyer, C.; Lasch-Born, P.; Suckow, F.; Gutsch, M.; Murawski, A.; Pilz, T. Projections of regional changes in forest net primary productivity for different tree species in Europe driven by climate change and carbon dioxide. *Ann. For. Sci.* **2014**, *71*, 211–225.
6. Farquhar, G.D.; Sharkey, T.D. Stomatal conductance and phostosynthesis. *Annu. Rev. Plant Physiol.* **1982**, *33*, 317–345.
7. Jarvis, A.J.; Davies, W.J. The coupled response of stomatal conductance to photosynthesis and transpiration. *J. Exp. Bot.* **1998**, *49*, 399–406.
8. Lindner, M.; Fitzgerald, J.B.; Zimmermann, N.E.; Reyer, C.; Delzon, S.; van der Maaten, E.; Schelhaas, M.J.; Lasch-Born, P.; Eggers, J.; van der Maaten-Theunissen, M.; *et al*. Climate Change and European Forests: What do we know, what are the uncertainties, and what are the implications for forest management? *J. Environ. Manag.* **2014**, *146*, 69–83.
9. Scarascia-Mugnozza, G.; Oswald, H.; Piussi, P.; Radoglou, K. Forests of the Mediterranean region: Gaps in knowledge and research needs. *For. Ecol. Manag.* **2000**, *132*, 97–109.
10. Breda, N.; Huc, R.; Granier, A.; Dreyer, E. Temperate forest trees and stands under severe drought: A review of ecophysiological responses, adaptation processes and long-term consequences. *Ann. For. Sci.***2006**, *63*, 625–644.

11. Galiano, L.; Martínez-Vilalta, J.; Lloret, F. Drought-Induced Multifactor Decline of Scots Pine in the Pyrenees and Potential Vegetation Change by the Expansion of Co-occurring Oak Species. *Ecosystems* **2010**, *13*, 978–991.
12. Poyatos, R.; Martinez-Vilalta, J.; Cermak, J.; Ceulemans, R.; Granier, A.; Irvine, J.; Kostner, B.; Lagergren, F.; Meiresonne, L.; Nadezhdina, N.; *et al*. Plasticity in hydraulic architecture of Scots pine across Eurasia. *Oecologia* **2007**, *153*, 245–259.
13. Rebetez, M.; Dobbertin, M. Climate change may already threaten Scots pine stands in the Swiss Alps. *Theor. Appl. Climatol.* **2004**, *79*, 1–9.
14. Cruiziat, P.; Cochard, H.; Ameglio, T. Hydraulic architecture of trees: Main concepts and results. *Ann. For. Sci.* **2002**, *59*, 723–752.
15. Holst, J.; Grote, R.; Offermann, C.; Ferrio, J.P.; Gessler, A.; Mayer, H.; Rennenberg, H. Water fluxes within beech stands in complex terrain. *Int. J. Biometeorol.* **2010**, *54*, 23–36.
16. Keenan, T.; Sabate, S.; Gracia, C. Soil water stress and coupled photosynthesis–conductance models: Bridging the gap between conflicting reports on the relative roles of stomatal, mesophyll conductance and biochemical limitations to photosynthesis. *Agric. For. Meteorol.* **2010**, *150*, 443–453.
17. Keenan, T.; Garcia, R.; Friend, A.D.; Zaehle, S.; Gracia, C.; Sabate, S. Improved understanding of drought controls on seasonal variation in Mediterranean forest canopy CO_2 and water fluxes through combined *in situ* measurements and ecosystem modelling. *Biogeosciences* **2009**, *6*, 1423–1444.
18. Wang, Y.; Bauerle, W.L.; Reynolds, R.F. Predicting the growth of deciduous tree species in response to water stress: FVS-BGC model parameterization, application, and evaluation. *Ecol. Model.* **2008**, *217*, 139–147.
19. Reyer, C.; Leuzinger, S.; Rammig, A.; Wolf, A.; Bartholomeus, R.P.; Bonfante, A.; de Lorenzi, F.; Dury, M.; Gloning, P.; Abou Jaoudé, R.; *et al*. A plant's perspective of extremes: Terrestrial plant responses to changing climatic variability. *Glob. Chang. Biol.* **2013**, *19*, 75–89.
20. Williams, M.; Rastetter, E.B.; Fernandes, D.N.; Goulden, M.L.; Wofsy, S.C.; Shaver, G.R.; Melillo, J.M.; Munger, J.W.; Fan, S.M.; Nadelhoffer, K.J.; *et al*. Modelling the soil-plant-atmosphere continuum in a Quercus-Acer stand at Harvard forest: The regulation of stomatal conductance by light, nitrogen and soil/plant hydraulic properties. *Plant Cell Environ.* **1996**, *19*, 911–927.
21. Campbell, G.S. Simulations of Water Uptake by Plant Roots. In *Modeling Plant and Soil Systems*; Hanks, J., Ritchie, J.T., Eds.; American Society of Agronomy: Madison, WI, USA, 1991; pp. 273–285.
22. Doussan, C.; Vercambre, G.; Pages, L. Modelling of the hydraulic architecture of root systems: An integrated approach to water absorption—Distribution of axial and radial conductances in maize. *Ann. Bot.* **1998**, *81*, 225–232.
23. Grant, R.F.; Arain, A.; Arora, V.; Barr, A.; Black, T.A.; Chen, J.; Wang, S.; Yuan, F.; Zhang, Y. Intercomparison of techniques to model high temperature effects on CO_2 and energy exchange in temperate and boreal coniferous forests. *Ecol. Model.* **2005**, *188*, 217–252.
24. Hacke, U.G.; Sperry, J.S.; Ewers, B.E.; Ellsworth, D.S.; Schäfer, K.V.R.; Oren, R. Influence of soil porosity on water use in Pinus taeda. *Oecologia* **2000**, *124*, 495–505.

25. Williams, M.; Bond, B.J.; Ryan, M.G. Evaluating different soil and plant hydraulic constraints on tree function using a model and sap flow data from ponderosa pine. *Plant Cell Environ.* **2001**, *24*, 679–690.
26. Williams, M.; Law, B.E.; Anthoni, P.M.; Unsworth, M.H. Use of a simulation model and ecosystem flux data to examine carbon-water interactions in ponderosa pine. *Tree Physiol.* **2001**, *21*, 287–298.
27. Grote, R.; Suckow, F. Integrating dynamic morphological properties into forest growth modeling. I. Effects on water balance and gas exchange. *For. Ecol. Manag.* **1998**, *112*, 101–119.
28. Kirschbaum, M.U.F. CenW, a forest growth model with linked carbon, energy, nutrient and water cycles. *Ecol. Model.* **1999**, *118*, 17–59.
29. Beniston, M. Weather and Climate Extremes: Where Can Dendrochronology Help? In *Tree Rings and Natural Hazards: A State-of-Art*; Stoffel, M., Bollschweiler, M., Butler, D.R., Luckman, B.H., Eds.; Springer: Dordrecht, The Netherlands; Heidelberg, Germany, 2010; pp. 401–413
30. Bugmann, H.; Grote, R.; Lasch, P.; Lindner, M.; Suckow, F. A new forest gap model to study the effects of environmental change on forest structure and functioning. Impacts of Global Change on Tree Physiology and Forest Ecosystems. In Proceedings of the International Conference on Impacts of Global Change on Tree Physiology and Forest Ecosystems, Wageningen, The Netherlands, 26–29 November 1996; Mohren, G.M.J., Kramer, K., Sabate, S., Eds.; Kluwer Academic Publisher: Dordrecht, The Netherlands, 1997; pp. 255–261.
31. Lasch, P.; Lindner, M.; Erhard, M.; Suckow, F.; Wenzel, A. Regional impact assessment on forest structure and functions under climate change—The Brandenburg case study. *For. Ecol. Manag.* **2002**, *162*, 73–86.
32. Haxeltine, A.; Prentice, I.C. BIOME3: An equilibrium terrestrial biosphere model based on ecophysiological constraints, resource availability and competition among plant functional types. *Glob. Biogeochem. Cycles* **1996**, *10*, 693–709.
33. Schaber, J.; Badeck, F.W. Physiology based phenology models for forest tree species in Germany. *Int. J. Biometeorol.* **2003**, *47*, 193–201.
34. Glugla, G. Berechnungsverfahren zur Ermittlung des aktuellen Wassergehaltes und Gravitationswasserabflusses im Boden. *Albrecht-Thaer-Archiv* **1969**, *13*, 371–376.
35. Koitzsch, R. Schätzung der Bodenfeuchte aus meteorologischen Daten, Boden- und Pflanzenparametern mit einem Mehrschichtmodell. *Z. Meteorol.* **1977**, *27*, 302–306.
36. DVWK. *Ermittlung der VERDUNSTUNG von Land- und Wasserflächen*; Wirtschafts- und Verlagsgesellschaft Gas und Wasser mbH: Bonn, Germany, 1996; p. 134.
37. Chen, C.W. The response of plants to interacting stresses: PGSM Version 1.3 Model Documentation (TR-101880); Report, OSTI ID: 6889091; Electric Power Research Institute: Palo Alto, CA, USA, 1993; p. 127.
38. VanGenuchten, M.T. A closed-form equation for predicting the hydraulic conductivity of unsaturated soils. *Soil Sci. Soc. Am. J.* **1980**, *44*, 892–898.
39. Granier, A. Une nouvelle méthode pour la mesure du flux de sève brute dans le tronc des arbres. *Ann. Sci. For.* **1985**, *42*, 193–200.

40. Lüttschwager, D.; Rust, S.; Wulf, M.; Forker, J.; Hüttl, R.F. Tree canopy and herb layer transpiration in three Scots pine stands with different stand structures. *Ann. For. Sci.* **1999**, *56*, 265–274.
41. Landeskompetenzzentrum Forst Eberswalde, Forstliche-Umweltkontrolle. Available online: www.forstliche-umweltkontrolle-bb.de/index.php (accessed on 19 May 2015).
42. Badeck, F.W.; Beese, F.; Berthold, D.; Einert, P.; Jochheim, H.; Kallweit, R.; Konopatzky, A.; Lasch, P.; Meesenburg, H.; Meiwes, K.-J.; *et al*. Parametrisierung, Kalibrierung und Validierung von Modellen des Kohlenstoffumsatzes in Waldökosystemen und deren Böden. DE 2003/2004 BB 5, DE 2003/2004 BY 4, DE 2003/2004 NI 6. F.F. C2-Projekte, Bayerische Landesanstalt für Wald und Forstwirtschaft (LWF), Institut für Bodenkunde und Waldernährung der Universität Göttingen (IBW), Landesforstanstalt Eberswalde (LFE), Leibniz-Zentrum für Agrarlandschaftsforschung (ZALF), Nordwestdeutsche Forstliche Versuchsanstalt (NW-FVA), Potsdam-Institut für Klimafolgenforschung (PIK): Potsdam, Germany, 2007; p. 110.
43. Meiwes, K.-J.; Badeck, F.W.; Beese, F.; Berthold, D.; Einert, P.; Jochheim, H.; Kallweit, R.; Konopatzky, A.; Lasch, P.; Meesenburg, H.; *et al*. Kohlenstoffumsatz in Waldökosystemen und deren Böden. Parametrisierung, Kalibrierung und Validierung von Modellen. *AFZ/Der Wald* **2007**, *20*, 1076–1078.
44. Beck, W. Growth patterns of forest stands—The response towards pollutants and climatic impact. *iForest* **2009**, *2*, 4–6.
45. Schröder, J.; Löffler, S.; Michel, A.; Kätzel, R. Genetische Differenzierung, Zuwachsentwicklung und Witterungseinfluß in Mischbeständen von Traubeneiche und Kiefer. *Forst Holz* **2009**, *64*, 18–24.
46. Maechler, M.; Rousseeuw, P.; Struyf, A.; Hubert, M.; Hornik, K. *Cluster Analysis Basics and Extensions. R Package*, Version 2.0.1. Available online: http://cran.r-project.org/web/packages/cluster/citation.html (accessed on 21 March 2015).
47. R Development Core Team. *R: A Language and Environment for Statistical Computing*; R Foundation for Statistical Computing: Vienna, Austria, 2009; ISBN 3-900051-07-0. Available online: http://www.R-project.org (accessed on 3 June 2015).
48. McGill, R.; Tukey, J.W.; Larsen, W.A. Variations of box plots. *Am. Stat.* **1978**, *32*, 12–16.
49. Coners, H. Wasseraufnahme und artspezifische hydraulische Eigenschaften der Feinwurzeln von Buche, Eiche und Fichte: *In situ*-Messungen an Altbäumen. Ph.D. Thesis, Mathematisch-Naturwissenschaftliche Fakultäten der Georg-August-Universität zu Göttingen, Göttingen, Germany, 2001.
50. Kostner, B.; Biron, P.; Siegwolf, R.; Granier, A. Estimates of water vapor flux and canopy conductance of Scots pine at the tree level utilizing different xylem sap flow methods. *Theor. Appl. Climatol.* **1996**, *53*, 105–113.
51. Wilson, K.B.; Hanson, P.J.; Mulholland, P.J.; Baldocchi, D.D.; Wullschleger, S.D. A comparison of methods for determining forest evapotranspiration and its components: Sap-Flow, soil water budget, eddy covariance and catchment water balance. *Agric. For. Meteorol.* **2001**, *106*, 153–168.
52. Bittner, S.; Talkner, U.; Kramer, I.; Beese, F.; Holscher, D.; Priesack, E. Modeling stand water budgets of mixed temperate broad-leaved forest stands by considering variations in species specific drought response. *Agric. For. Meteorol.* **2010**, *150*, 1347–1357.

53. Granier, A.; Loustau, D. Measuring and Modeling the transpiration of a maritime pine canopy from sap-flow data. *Agric. For. Meteorol.* **1994**, *71*, 61–81.
54. Lundblad, M.; Lindroth, A. Stand transpiration and sapflow density in relation to weather, soil moisture and stand characteristics. *Basic Appl. Ecol.* **2002**, *3*, 229–243.
55. Hanson, P.J.; Amthor, J.S.; Wullschleger, S.D.; Wilson, K.B.; Grant, R.F.; Hartley, A.; Hu, D.; Hunt, J.E.R.; Johnson, D.W.; Kimball, J.S.; *et al*. Oak forest carbon and water simulations: Model intercomparisons and evaluations against independent data. *Ecol. Monogr.* **2004**, *74*, 443–489.